COMPOSITE STIFFENED PANELS IN POSTBUCKLING: EXPERIMENTS AND DYNAMIC EXPLICIT ANALYSES WITH LS-DYNA

Luca Lanzi*
Dipartimento di Ingegneria Aerospaziale - Politecnico di Milano
Via La Masa 34, 20156 Milano, Italy

Abstract

This research investigates the postbuckling behaviour of composite stiffened panels under axial compression up to collapse. Two different panel configurations are designed to operate in post-buckling, namely a flat panel and a low curvature panel configuration. Finite element analyses are performed with Ls-Dyna, a commercial finite element explicit code widely used in engineering for impact and crashworthy applications, as well as for highly non linear structural problems. After an accurate characterisation of the material properties, the load vs. shortening curves and the deformed shape evolution from the pre-buckling to the post-buckling until structure collapse are numerically investigated. Thereafter, numerical results are compared to experimental tests carried out considering two specimens for each panel configuration. The obtained results are in good agreement with respect to the equilibrium path and of the out-of-plane deformations. Interesting considerations are carried out with respect to the failure mechanisms that mainly involve the panel stiffeners and bring to structural collapse. When the low curvature panel configuration has been considered, the introduction of initial geometrical imperfections, which were measured during the experimental activities, has significantly improved the numerical-experimental correlation on the buckling loads.

Introduction

Composite materials appear extremely performing due to their high strength-to-weight and high stiffness-to-weight ratios. Indeed, they have been already extensively used in some aircraft structures achieving significant reduction of the structural weight, without reducing structural life and structural safety.

Unfortunately, the weight saving capabilities of composite materials seems nowadays not completely exploited especially because structures actually manufactured using composite materials are not expressively designed to undergo post-buckling loads.

Recent experiments and numerical studies (Ref 1-7) have shown that further weight savings could be achieved allowing stiffened composite structures to work in post-buckling field.

In the last years, the improvements in computational methods made available more sophisticated numerical models, capable to correctly predict the post-buckling response of shells, allowing to investigate complex geometries, loading and boundary conditions, as well as to model initial geometric imperfections. These computational methods have been already used to perform structural optimization of composite panels under buckling, post-buckling and strength constrains (Ref 8-10).

Dynamic analyses appear only recently to investigate buckling phenomena. Nowadays, they represent an attractive alternative to the classical finite element approaches based on eigenvalues and static analysis. As a matter of fact, numerical models have to be validated with test results, before they can be also used with enough confidence. Numerical models could be used also in this validation task to select and design ad hoc experiments as well as to better understand the effects of different and non-ideal test conditions. This selective test approach is particularly important considering the costs and the time required by the experiments.

This research is part of a larger European project, "POSICOSS – Improved Post-buckling Simulation for Design of Fibre Composite Stiffened Fuselage Structures", that aims at improving the knowledge on the buckling and post-buckling behaviour of composite stiffened shell structures.

Numerical analyses and experiments are performed up to collapse considering two different configurations of composite stiffened panels: a flat panel configuration and a low curvature panel configuration. Both the panel configurations have been expressively designed to operate in postbuckling.

The use of explicit finite element analyses is investigated with particular attention to the effects of the displacement velocity imposed to the upper edge of the panels to provide its axial compression. Finite element analyses were performed using the

*Corresponding author: Luca Lanzi
        e-mail:
        phone: +39 02 2399 8365

commercial finite element explicit code Ls-Dyna (Ref 11), version 950. Ls-Dyna is an explicit finite element code widely used in engineering for impact and crashworthy applications, as well as for highly non linear structural problems.

Two distinct specimens for each panel configuration are manufactured by AGUSTA using a CFRP woven and tested at *Politecnico di Milano* after the initial geometrical imperfections have been measured. Experimental results are finally compared with the numerical computations.

Panel configurations

Two different panel configurations are here considered: a flat panel configuration and a low curvature panel with nominal radius of 1500 *mm*. Both the configurations present free length and width of 700 *mm*. They are characterised by 6 L-shaped stiffeners, 28 *mm* wide. The stiffeners are equally spaced along the panel width. The first and the last stiffeners are located in compliance with the lateral edges of the panel skin. In this way, premature buckling localised on the lateral edges of the panel skin is prevented during experimental tests.

The stiffener lay-up of the flat panel consists of $[0°/90°]_S$ oriented layers, while that of the shallow panel consists of 9 layers, 0° and 90° alternatively oriented. Both the panel configurations have a 4 layers skin: the layers of the flat panel configuration are $[45°/0°]_S$ oriented, while those of the low curvature panel are $[0°/45°]_S$ oriented.

All the panels are made of the same composite woven material: CYNAMID 98-GF3-5H1000.

In order to correctly evaluate the mechanical properties of the material, an experimental characterisation was carried out via static tests on small specimens. The specimens were manufactured by AGUSTA. Experimental tests were performed according to the IEPG-CTP-TA 21 (Ref 12) guidelines at the *Dipartimento di Ingegneria Aerospaziale* of Politecnico di Milano.

Numerical computations

The load vs. shortening curve and the investigation of the deformed shape evolution from the pre-buckling to the postbuckling, until structure collapse, are obtained by dynamic analyses. Dynamic analyses are based on equilibrium equations which directly consider inertial forces and time-dependent phenomena.

Dynamic analyses, using both implicit and explicit time-integration solvers, recently appeared within the numerical methods applied in investigating buckling problems and they have now become an attractive alternative to the usual finite element eigenvalues and static analyses.

In this work, since neither reliable statistical data, nor preliminary estimation of possible magnitude and shape of initial geometrical imperfections were available during the design phase, the geometry of the structures was assumed to be perfect.

Model characteristics: the structures have been modelled using 4-node shells, with six degrees of freedom at each node and three integration points throughout the thickness for each composite ply. Following a preliminary sensitivity study on the element size, the dimensions of the shell elements were chosen equal to 8x8 *mm*.

In order to reproduce the experimental conditions as accurately as possible, finite element analyses are performed by fixing the lower edge of the panel and imposing a known displacement to the upper one with a constant displacement velocity.

Skin-stiffener connections: it was decided to model the panel skin and the stiffeners separately as shown in Figure 1. The adopted solution allows to consider the real thickness and the relative position of the skin with respect to the stiffeners. Panel skin and stiffener flanges are then jointed by means of generalised spot-weld constraints.
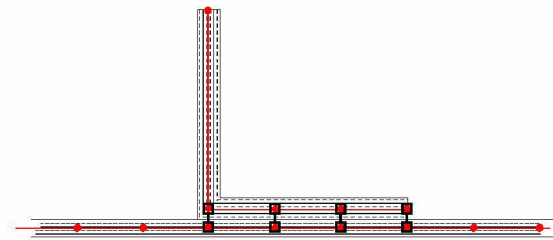

Figure 1: Stiffener-skin connection model.

Material model: in finite element computations, the same average elastic modulus is defined both along fibre and orthogonal directions. Similar considerations are done with respect to the strength properties. The material properties used in the finite element analyses are reported in Table 1.

Table 1: Mechanical properties used in the numerical computations.

Description	Value
Elastic modulus $E_{11} = E_{22}$	55700 *[N/mm²]*
Poisson coefficient $v_{12}=v_{21}$	0.048
Shear modulus $G_{12}= G_{13}= G_{23}$	3060 *[N/mm²]*
Tensile strength $\sigma_{11} = \sigma_{22}$	431 *[N/mm²]*
Compression strength $\sigma_{11} = \sigma_{22}$	467 *[N/mm²]*
Shear in plane strength τ	99 *[N/mm²]*
Ply thickness	0.33 *[mm]*

The material model MAT 58 (Ref 11) is used. It is especially developed for laminated composite material: the damage model has been developed considering that the deformations introduce micro-cracks and cavities into material and these defects primarily cause stiffness degradation with rather small permanent deformation.

The material model MAT 58 also allows to model the non-linear shear behaviour of composite materials. For this reason, the numerical $\tau(\gamma)$ curve has been tuned on the base of the results obtained during the material characterisation.

Figure 2 shows the in-plane shear stress-strain curves obtained during tests and computation, respectively.
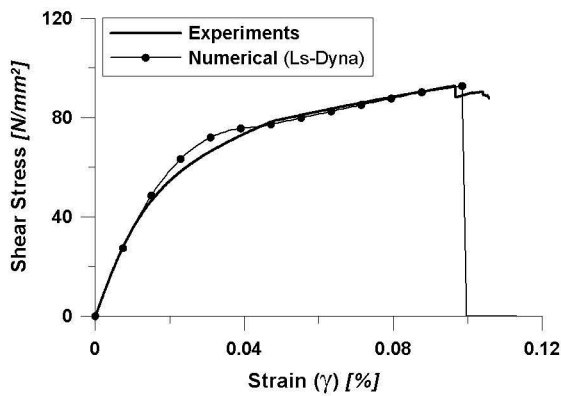
Figure 2: Numerical and experimental in-plane shear stress-strain curve.

Following the above guidelines, the flat and low curvature panels have been modelled by using 8094 nodes and 7490 shell elements. A total number of 1464 spot-weld were used to connect the panel skin to the stiffeners flanges.

Flat panel

The following section presents the numerical results obtained with the flat panel configuration, particular emphasising the effects of the displacement velocity of the upper edge on the buckling and post-buckling behaviour.

Effects of the displacement velocity: An investigation on the effects of the displacement velocity in the calculations of buckling phenomena is carried out. In fact, as previous works (Ref 9) proved, the value of the displacement velocity is of primary importance to obtain reliable buckling and post-buckling evaluations using dynamic analyses.

Dynamic explicit analyses are then performed changing the displacement velocity of the upper edge of the panel. Displacement velocities equal to 200 *mm/s*, 100 *mm/s*, 50 *mm/s*, 10 *mm/s* and 5

mm/s have been considered. The obtained load-displacement curves are compared in Figure 3 while buckling loads, collapse loads and CPU times required to reach an end shortening of 2.0 *mm* are compared in Table 2 and Figure 4.
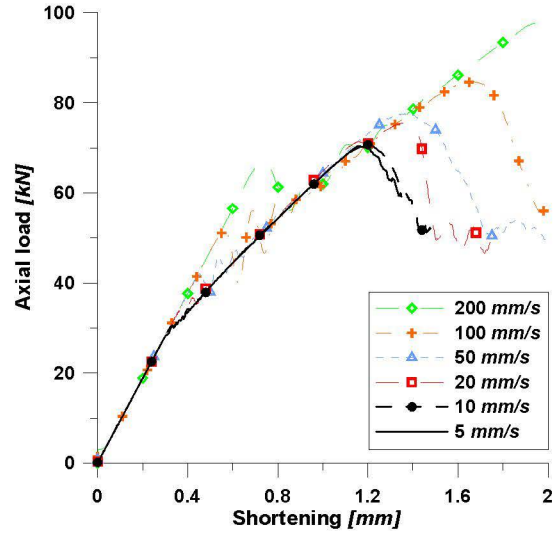

Figure 3: Load-shortening curves for different displacement velocities.
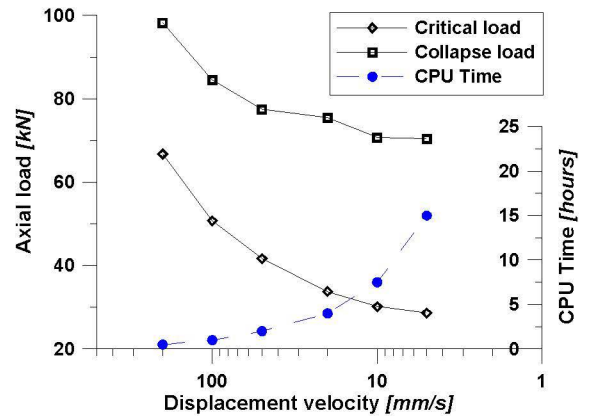

Figure 4: Buckling load, collapse load and CPU time for different displacement velocities.

Table 2: Sensitivity of the results to the displacement velocity.

Displacement velocity	Critical load *[kN]*	Collapse load *[kN]*	CPU time* (hours)
200 *[mm/s]*	66.78	98.2	0.5
100 *[mm/s]*	50.72	84.5	1
50 *[mm/s]*	41.67	77.46	2
20 *[mm/s]*	33.77	75.45	4
10 *[mm/s]*	30.16	70.7	7
5 *[mm/s]*	29.8	70.4	14

[*] on a Pentium IV 1.5GHz processor with 512Mb of RAM memory.

The parametric study shows that the use of excessively high values of the displacement velocity in the numerical modelling of quasi-static phenomena, such as the buckling ones, may lead to overestimations of the stability performances of the structure. In fact, higher values, both of the buckling loads and of the collapse loads, are obtained when the displacement velocity is increased.

In particular, referring to Figure 3, inertial effects do not effect the initial stiffness. On the other hand, numerical analyses performed with a displacement velocity equal to the one typically used in experimental tests will turn out to be unaffordable from a computational point of view, requiring an enormously high computation time.

Therefore, a preliminary convergence study on the displacement velocity seems a prerequisite to obtain reliable results using dynamic analyses and to contain the simulation time as much as possible without loss of result reliability. Limiting to the structural typologies investigated in this work, the convergence study suggests to use a displacement velocity equal to 5 *mm/s*.

Buckling and postbuckling behaviour: The load vs. shortening curve and the deformed shape evolution of the flat panel configuration are investigated considering as reference analysis the one performed with the displacement velocity of 5 *mm/s*. The results of this analysis are summarized in Table 3.

The value of the first buckling load has been identified on the equilibrium path by a slope decrease of the load-shortening curve, i.e. a decrease of the structural stiffness at a value of about 29.8 *kN*.

The panel configuration shows good capabilities to undergo increasing loads without important gaps and discontinuities on the equilibrium path, as shown in
Figure 5.

In fact, even when the first buckling load has been overcome, the load-shortening curve seems to increase linearly, even in post-buckling range until the structural collapse, which takes place due to stiffener instability.

Table 3: Numerical behaviour of the flat panel configuration.

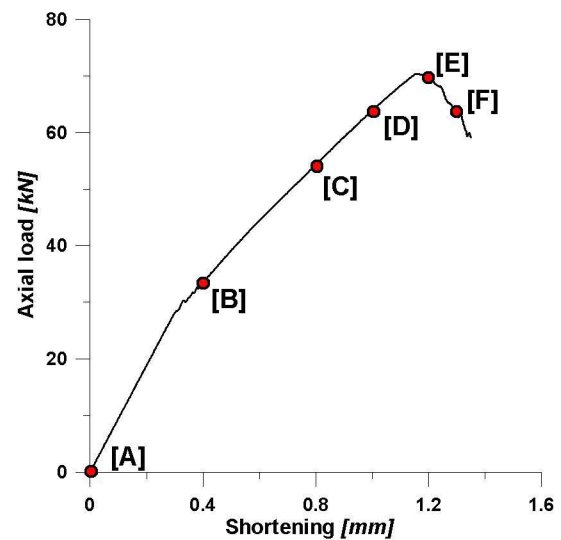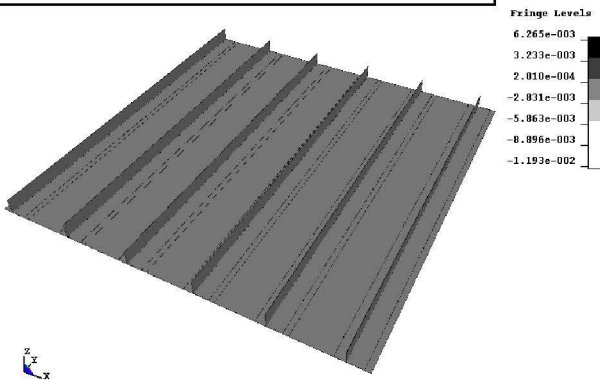|	
First buckling load *[kN]*	29.8
Shortening at the first buckling load *[mm]*	0.33
Initial pre-buckling stiffness *[kN/mm]*	91.1
Initial post-buckling stiffness *[kN/mm]*	51.2
Collapse load *[kN]*	70.4
Shortening at the collapse load *[mm]*	1.20

Figure 5: Numerical load-shortening curve of the flat panel configuration, displacement velocity of 5 *mm/s*.

[A] Axial load: 0.0 *kN* - Shortening: 0.00
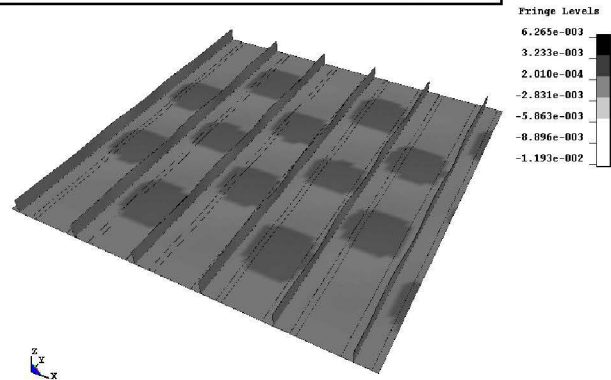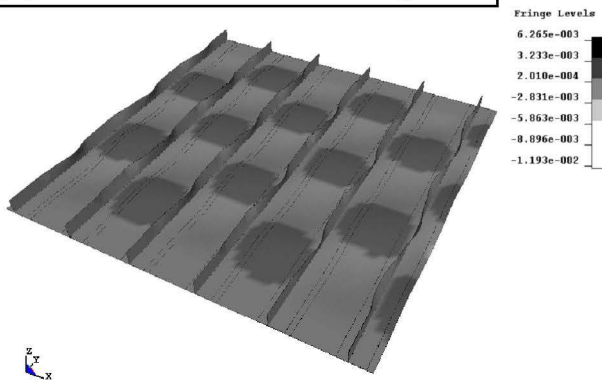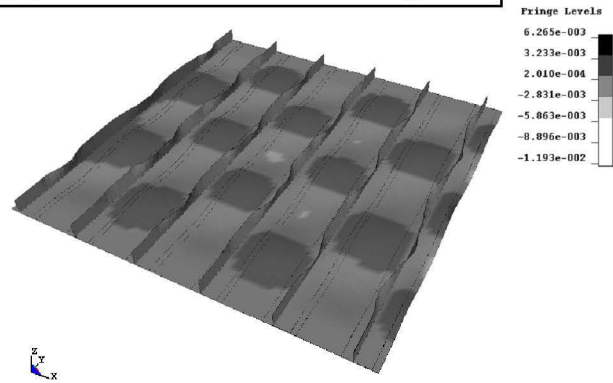
[B] Axial load: 34.2 *kN* - Shortening: 0.40

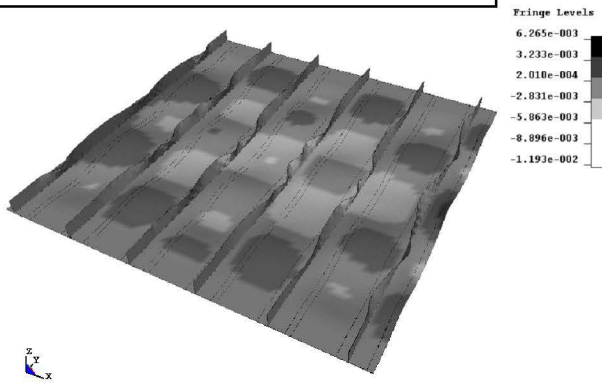Figure 6: Out of plane deformations numerically computed by Ls-Dyna.

[C] Axial load: 54.5 *kN* - Shortening: 0.80

[D] Axial load: 63.9 *kN* - Shortening: 1.00

[E] Axial load: 70.7 *kN* - Shortening: 1.20

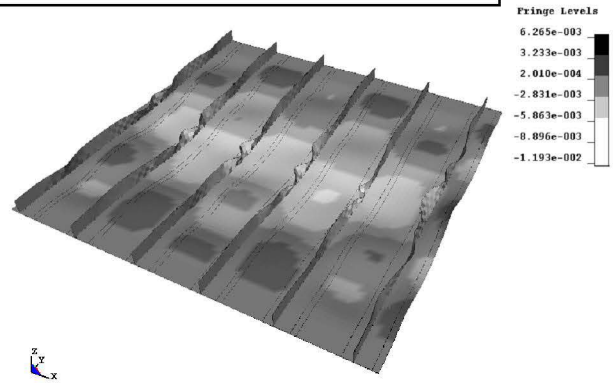[F] Axial load: 66.8 *kN* - Shortening: 1.30

Figure 7: Out of plane deformations numerically computed by Ls-Dyna and collapse modalities.

The postbuckling pattern is characterized by five half waves in the vertical direction and five half waves in the horizontal direction, as depicted in Figure 6. The waves are laterally limited by the presence of the stiffeners. The buckling shape remains stable during the whole postbuckling field and no changes in the buckling modes are numerically observed as shown in Figures 6 and 7. Structural collapse takes place due to the failure of the stiffeners because of their high bending and shear deformations. Results obtained by the dynamic explicit analysis point out that failures are localised at the stiffener blades at half of the panel free length. In any case, the panel seems capable of exploiting a widely large postbuckling range before the collapse.

Low curvature panel

Basing on the parametric studies above discussed and concerning the displacement velocity, the buckling and postbuckling behaviour of the low curvature panel configuration has been investigated by means of a dynamic explicit finite element analysis with displacement velocity of 5 *mm/s*.

The obtained load-shortening curve is reported in Figure 8, while the analysis results are summarized in Table 4.
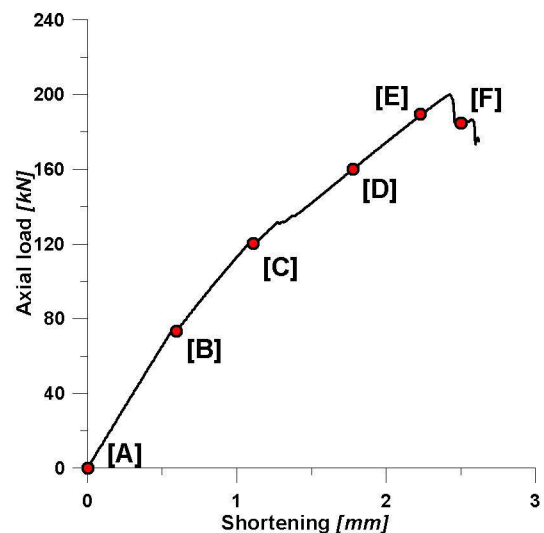
Figure 8: Numerical load-shortening curve of the low curvature panel configuration, displacement velocity of 5 *mm/s*.

5

First buckling load [kN]	73.2
Shortening at the first buckling load [mm]	0.58
Initial pre-buckling stiffness [kN/mm]	126
Initial post-buckling stiffness [kN/mm]	97
Collapse load [kN]	198.8
Shortening at the collapse load [mm]	2.44

The first buckling load has been experienced in corresponding of an axial load of 73.2 kN. The buckling pattern remains limited to the panel skin and produces a controlled decrease of the structural stiffness, without significant load gaps.

Large part of the postbuckling range is characterized by an almost linear behaviour and the reduction of the axial stiffness due to the local skin instability is about 24%, corresponding to an initial postbuckling stiffness of about 97 kN.

The buckling pattern evolves from an irregular map to a much more regular map of five half waves in each panel sector. It seems completely developed at axial load of 120 kN is reached, as shown in Figure 9. Thereafter, it remains stable up to collapse.

As it has been observed for the flat panel configuration, the instabilities localised at the blades of the stiffeners lead to the structural collapse. The collapse pattern seems asymmetric and is characterised by a sudden change of the structure shape throughout the development of a main wave localised to the right part of the panel and extended to the central vertical sectors, as shown in Figure 10.
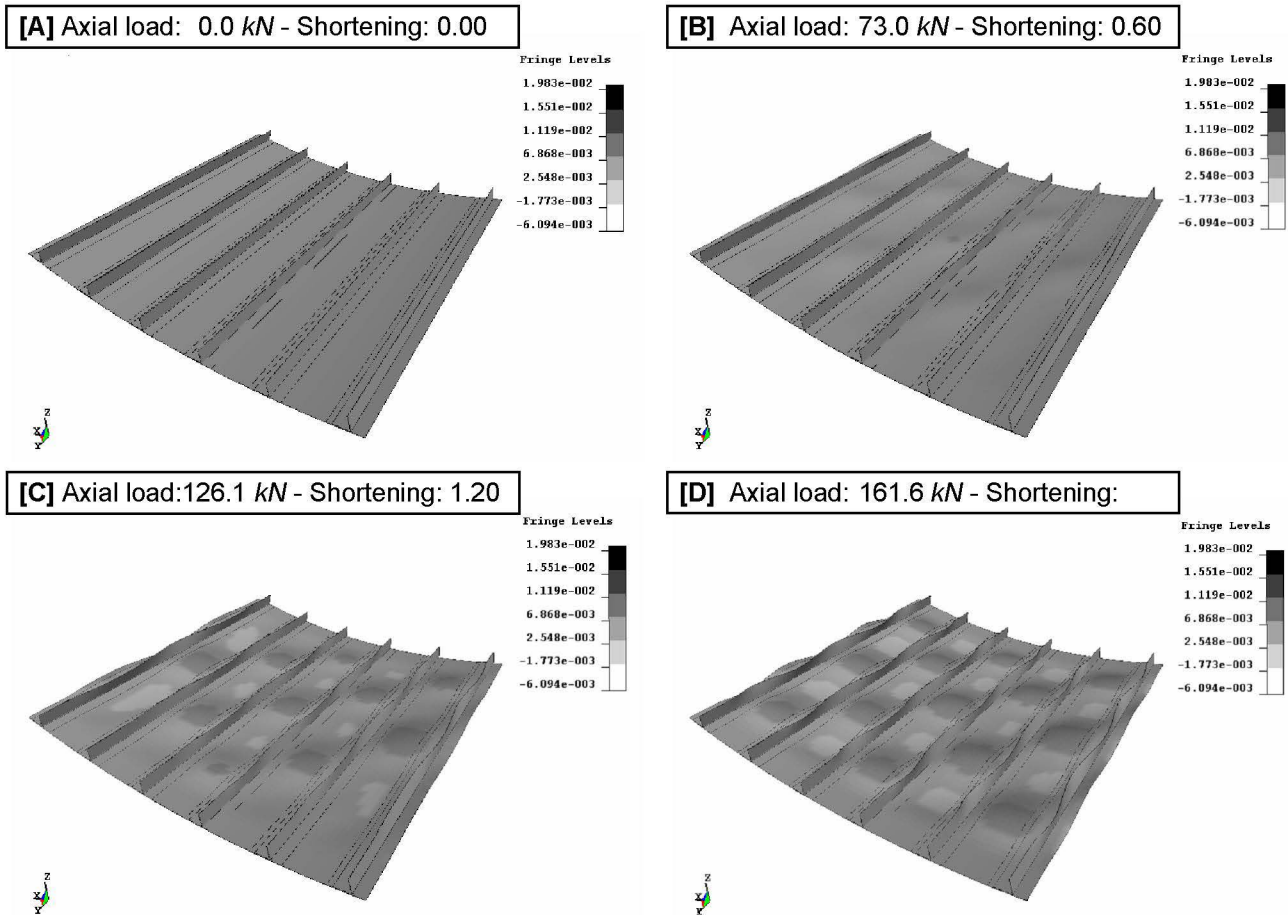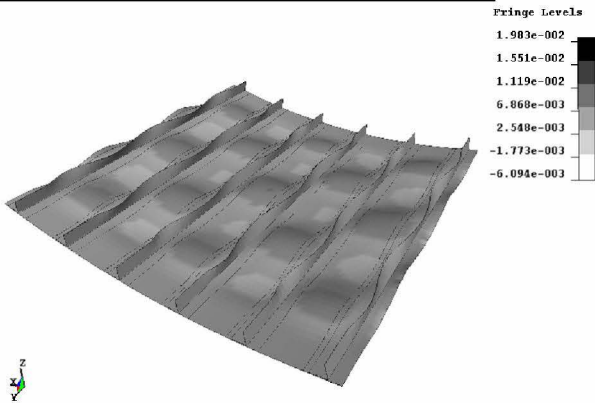

Figure 9:   Out of plane deformation numerically computed by Ls-Dyna.

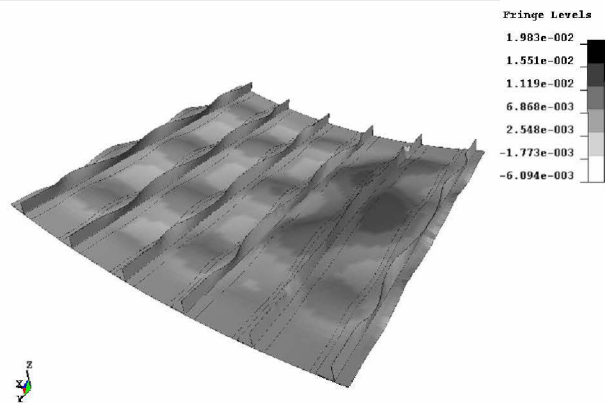| [E] Axial load: 186.9 *kN* - Shortening:	[F] Axial load: 187 *kN* - Shortening: 2.50

Figure 10: Out of plane deformation numerically computed by Ls-Dyna and collapse modalities.

Numerical-Experimental correlation

AGUSTA manufactured two specimens for each one of the previously described configurations, namely specimens **P1** and **P2** for the flat panel configuration, specimens **P3** and **P4** for the low curvature panel configuration.

Since neither reliable statistical data, nor preliminary estimation of initial geometrical imperfections were available, it was decided to measure the initial shape of all the available specimens. The measurement of imperfections is limited to the unstiffened surface of the panel skin and is performed by using a displacement controlled probe.

Thereafter, axial compression tests have been performed up to the structure collapse. These collapse tests were performed by applying a controlled displacement with a shortening velocity equal to 0.05 *mm/s*; the out-of-plane deformations of the panel skin were visualized by using the shadow Moiré optical technique and recorded in real time by a high resolution digital camera. Strain-gauges were also located on the low curvature panels to precisely identify the first buckling load.

A detailed description of the experimental activities, of the results obtained, as well as of the test procedure and equipment are provided in Ref 8, 9 and 13. In this work, only few data related to the final experimental load-shortening curves and the postbuckling patterns are reported to be compared with the numerical analyses.

Flat panels

Figure 11 shows a comparison between the load-shortening curves experimentally obtained on the flat panels **P1** and **P2** and the numerical ones obtained with Ls-Dyna.
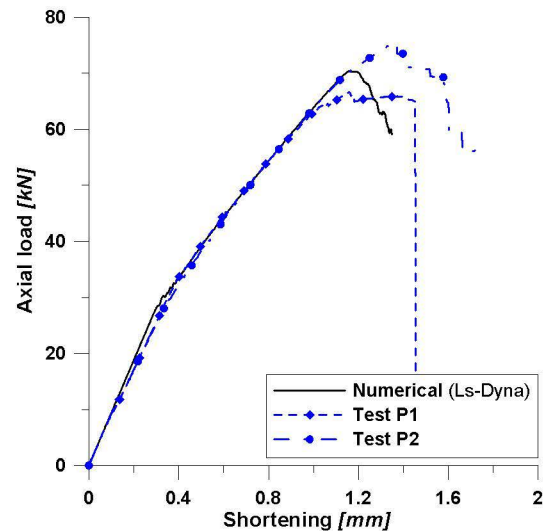

Figure 11: Numerical-experimental correlation on the load-shortening curves of the flat panel configuration.

Table 5: Numerical-experimental correlation on the flat panel configuration.

	Test **P1**	Test **P2**	Ls-Dyna
First buckling load [kN]	32.86	29.76	29.8
Shortening at the first buckling load [mm]	0.39	0.36	0.33
Initial pre-buckling stiffness [kN/mm]	83.71	83.45	91.1
Collapse load [kN]	66.7	75.4	70.4
Shortening at the collapse load [mm]	1.17	1.37	1.20

7

Table 5 summarises experimental and numerical results, whereas Figure 12 shows the comparison between the out of plane deformations as visualised by the Moirè fringes and as returned by the numerical analysis. The behaviour of the two specimens is very close in the pre-buckling field, while some differences related to the first buckling loads, the postbuckling behaviour and the collapse loads have been observed.

As evidenced by the numerical computations, the pre-buckling field is characterized by progressive out-of-plane deformations that suddenly change in a regular pattern of waves, once the first buckling load is reached. For both panels, the post-buckling regime is characterized by five half waves in the vertical direction for each panel sector.
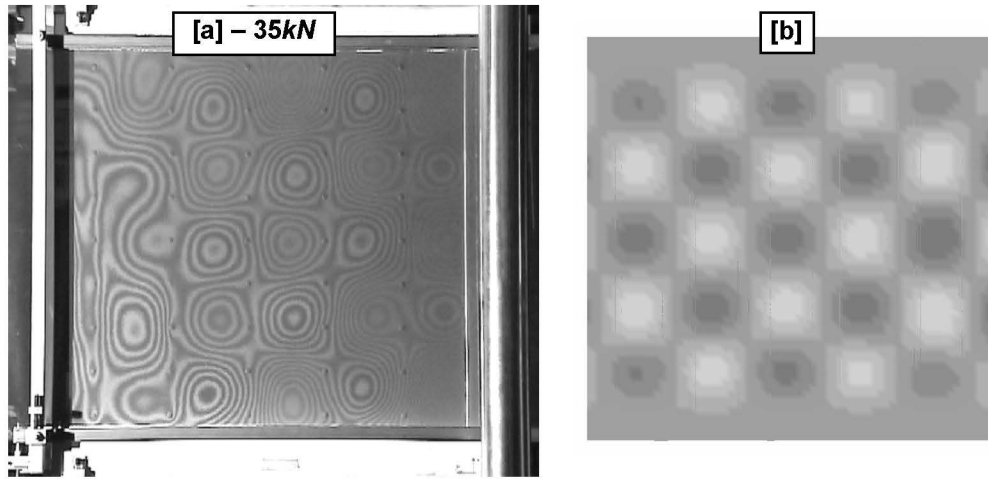

Figure 12: Out of plane deformations visualised by the Moiré shadow [a] and computed by Ls-Dyna [b], post buckling field of the flat panel configuration.

Low curvature panels

Perfect model: as previously done for the flat panel configuration, in Figure 13 the numerical load-shortening curve is superimposed to those experimentally obtained in the collapse tests of panels **P3** and **P4**, respectively.
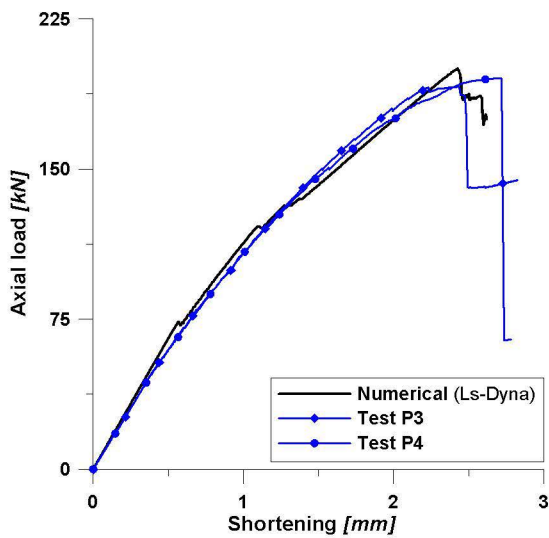

Figure 13: Numerical-experimental correlation on the low curvature panel configuration.

Table 6: Numerical-experimental correlation on the low curvature panel configuration.

	Test **P3**	Test **P4**	Ls-Dyna
First buckling load [kN]	55.5	59.2	73.2
Shortening at the first buckling load [mm]	0.44	0.47	0.58
Initial pre-buckling stiffness [kN/mm]	124	124	128
Collapse load [kN]	192	195	199
Shortening at the collapse load [mm]	2.22	2.72	2.44

Numerical and experimental results are compared in Table 6 while Figure 14 shows the out of plane deformations as visualised by the Moirè fringes and as returned by the numerical analyses.

A good correlation has been obtained on the number of waves and their shape as well as on their amplitude and direction. Indeed, hills and valleys were correctly identified for both tested panels.

As pointed out by the numerical analyses, local instabilities, involving only the blades of the stiffeners, were observed when the load exceeded a value of about 120 kN.
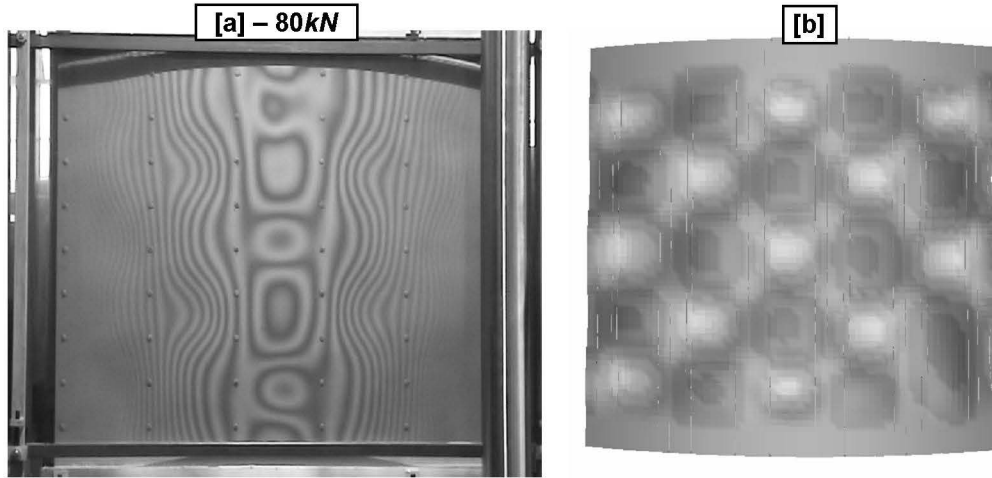
Figure 14:   Out of plane deformations visualised by the Moiré shadow [a] and computed by Ls-Dyna [b], post buckling field of the low curvature panel configuration.

Even if a satisfactory numerical-experimental correlation was obtained in terms of equilibrium path, out-of-plane deformations and failure modalities, a discrepancy on the first buckling loads is observed. Indeed, the first buckling loads which have been experienced during the tests are significantly lower than those numerically evaluated.

This discrepancy is probably due to the presence of initial geometrical imperfections.

Imperfect model: the geometrical imperfections measured during the experimental activities are then introduced in the numerical model. Consequently, two distinct models have been considered; one for each tested panel. The results obtained by these new imperfect models are summarized in Tables 7 and 8.

The introduction of the initial imperfections seems capable of improving the prediction of the pre-buckling behaviour leading to a significant reduction of the first buckling load. This reduction is probably explained by the shape of the initial geometrical imperfections which are significantly greater than the nominal thickness of the panel skin producing a gradual reduction of the panel curvature.

Apparently, the introduction of the imperfections contains the percentage errors between the numerical models and the experiments within 6.7% for the buckling loads and within 1% for the collapse loads.

Table 7:   Numerical-experimental correlation on the low curvature panel **P3** after the introduction of the initial geometrical imperfections.

	Test **P3**	Ls-Dyna	
		imperfect	Perfect
First buckling load *[kN]*	55.5	58.2	73.2
Shortening at the first buckling load *[mm]*	0.44	0.45	0.58
Initial pre-buckling stiffness *[kN/mm]*	124	128	128
Collapse load *[kN]*	192	190	199
Shortening at the collapse load *[mm]*	2.22	2.27	2.44

Table 8:   Numerical-experimental correlation on the low curvature panel **P4** after the introduction of the initial geometrical imperfections.

	Test **P4**	Ls-Dyna	
		imperfect	perfect
First buckling load *[kN]*	59.2	57.4	73.2
Shortening at the first buckling load *[mm]*	0.47	0.45	0.58
Initial pre-buckling stiffness *[kN/mm]*	124	128	128
Collapse load *[kN]*	195	193	199
Shortening at the collapse load *[mm]*	2.72	2.34	2.44

9

Conclusive remarks

Experimental tests and numerical analyses considering the post-buckling behaviour of composite stiffened panels are here presented.

The parametric study carried out on the flat panel configuration shows that the use of excessively high values of displacement velocity in the numerical modelling of quasi-static phenomena, such as the buckling ones, may lead to overestimations of the stability performances of the structure. Accordingly, after a sensitivity analysis, the displacement velocity has been fixed at 5 *mm/s*. The load-shortening curves obtained by numerical analyses with this displacement velocity are close and in good agreement with experimental data. Indeed, both the pre-buckling and post-buckling stiffness are correctly predicted by numerical analyses.

A good correlation is also obtained in terms of the out-of-plane deformations, of the shape and the dimensions of buckling waves. Indeed, waves on the skin side opposite to the stiffeners and waves on the stiffeners size are correctly identified in all the considered panels.

Interesting considerations are carried out in terms of failure mechanisms which mainly involve the panel stiffeners bringing structural collapse.

When the low curvature panels are considered, the introduction of initial geometrical imperfections reduced the percentage error between the numerical model and the tests within 7% with respect to the buckling and collapse loads.

Acknowledgement

References

1. Stiftinger MA, Skrna-Jakl IC, Rammerstorfer FG. "Buckling and post-buckling investigation of imperfect curved stringer-stiffened composite shells". *Thin-Walled Structures* 1995; 23:339-350.
2. Stevens KA, Ricci R, Davies GO. "Buckling and postbuckling of composite structures". *Composites: Part B* 1995; 26:189-199.
3. Falzon BG, Stevens KA, Davies GO. "Postbuckling behaviour of a blade-stiffened composite panel loaded in uniaxial compression". *Composites: Part A* 2000; 31:459-468.
4. Park O, Haftka RT, Sankar BV, Starnes JH Jr, Nagendra S. "Analytical-experimental correlation for a stiffened composite panel loaded in axial compression". *Journal of Aircraft* 2001; 38(2):379-387.
5. Chiarelli M, Lancetti A, Lanzotti L. "Compression behaviour of flat stiffened panels made of composite material". *Composite Structures* 1996; 36:161-169.
6. Weller T, Singer J. "Durability of stiffened composite panels under repeated buckling". *International Journal of Solids Structures* 1990; 26(9):1037-1069.
7. Abramovich H, Singer J, Weller T. "Repeated buckling and its influence on the geometrical imperfections of stiffened cylindrical shells under combined loading". *Int. J. Non-Linear Mechanics* 2002; 37:577-588.
8. Lanzi L, Bisagni C. "Post-Buckling experimental tests and numerical analyses on composite stiffened panels". *44th AIAA/ASME/ASCE/AHS Structures, Structural Dynamics, and Materials Conference*. 7-11 April 2003, Norfolk, USA.
9. Lanzi L. "Optimisation of composite stiffened panels under post-buckling constraints". *PhD Thesis. Dept. of Ingegneria Aerospaziale – Politecnico di Milano*, 2004.
10. Rikards R, Abramovich H, Auzins J, Korjakins A, Ozolinsh O, Kalnins K, Green T. "Surrogate models for optimum design of stiffened composite shells" *Composite Structures* 2004; 63:243-251.
11. Hallquist JO. LS-DYNA Theoretical Manual. *Livermore Software Technology Corporation*, 1998.
12. IEPG-CTP-TA 21 test guidelines, Collection of Test Methods and Related Tools, 1989.
13. Lanzi L. "An experimental investigation on the post-buckling behavior of composite stiffened panels", *45th AIAA/ASME/ASCE/AHS Structures, Structural Dynamics, and Materials Conference*. 19-22 April 2004, Palm Spring, USA.